

Nucleating Agents to Enhance Poly(L-lactide) Crystallization and Melting Behavior of Modified Poly(L-lactide)

HAO HUANG¹, JIE WU², YANHUA CAI^{1*}, JIE CHENG¹, LIN ZHANG¹, LISHA ZHAO¹

¹Chongqing Key Laboratory of Environmental Materials & Remediation Technologies, College of Chemistry and Environmental Engineering, College of Pharmaceutical Sciences, Chongqing University of Arts and Sciences, Chongqing-402160, P.R. China

²Sunyes Shanshan Advanced Materials Technology (Quzhou) Co, Ltd, Zhejiang-324000, P.R. China

Abstract: Melt processing poly(L-lactide) (PLLA) with a nucleating agent has been thought to be one of the most effective route to enhance PLLA's crystallization and heat resistance. In the current work, a newly-developed organic nucleating agent named N, N'-bis(2-picolinyl) 1, 4-naphthalenedicarboxylic acid dihydrazide (NCAPH) was synthesized to investigate its effects on PLLA's crystallization and melting behaviors. It is proved that NCAPH as an organic crystallization nucleating agent could provide large number of crystallization nucleation sites to improve PLLA's crystallization, as observed from DSC and POM measurements. The result from melt-crystallization processes further showed that the final melting temperature and cooling rate were two important factors for affecting PLLA's melt-crystallization behaviors in cooling, and the theoretical calculation result of frontier orbital energy indicated there existed probable intermolecular interaction between N-H of NCAPH and C=O of PLLA, which was proposed as nucleation mechanism of NCAPH for promoting PLLA's crystallization. The melting behaviors of PLLA/NCAPH after non-isothermal crystallization or isothermal crystallization further confirmed the positive effects of NCAPH and NCAPH's loading for the crystallization of PLLA, meantime, the melting behaviors depended on the heating rate, crystallization temperature, crystallization time, etc.

Keywords: nucleating agent, Poly(L-lactide), melt-crystallization, hydrazide, DSC

1. Introduction

The significant amount consumption of fossil fuel resources and serious "white pollution" problem are increasing the interest in biodegradable plastics like poly(L-lactide) (PLLA), polycaprolactone (PCL) and polyhydroxyalkanoates (PHA), and usage of these biodegradable polymers as substitutes for petroleum-based plastics can effectively solve the plastics pollution problem. Nowadays, in term of production capacity and application, PLLA is thought to be one of the most promising biodegradable polymer because of its renewable origin [1], high transparency [2], excellent thermoplastic processability [3], excellent mechanical strength and low in cost comparable to petroleum-based polymers [4], as well as excellent biodegradability and biocompatibility [5]. Moreover, with growing demand for biodegradable sustainable materials, the industry leadership of PLLA has been continuously strengthened. As a result, PLLA is applied in more various fields like textile [6], straw [7], temporary plugging agent [8], drug carrier [9] and diverting agent [10], it is these new applications that further accelerate the improvement of PLLA's capacity and application prospects.

Nevertheless, PLLA's some inherent defects, including low vicat softening temperature of about 60°C [11], slow crystallization rate [4], brittleness [2] and low melt strength [12, 13], significantly hinder its widespread adoption in daily life and industry. Adding nucleating agent, as one of the most efficient and common way, can enhance PLLA's nucleation process by lowering the surface energy barrier and increasing nucleation sites, potentially addressing the aforementioned limits in heat resistance and crystallization performance, because an increase of crystallinity must cause the modified PLLA to possess higher heat resistance during manufacturing, and this is an important strategy for enterprises to produce PLLA products with high heat resistance.

*email: caiyh651@aliyun.com

Numerous nucleating agents, for example, hydrazide compounds [14-16], amide compounds [17-19], clay [20-23], carbon nucleating agents [24-27], inorganic salt [28-30], have been used to enhance PLLA's melt nucleation rate. Especially nucleating agent with organic structure has huge demand in the recent years owing to its designability of organic structure, relatively better compatibility with PLLA matrix compared to inorganic nucleating agent, and increasing market share in PLLA nucleating agent industry. Our and other research groups have developed and studied various organic nucleating agents based on different organic molecular structures [31-38], as a typical example, Li *et al* [39] synthesized a good nucleating agent named furan-phosphamide derived from furfurylamine and phosphorus oxychloride, and upon the addition of 5 wt% furan-phosphamide in PLLA matrix, the half-time of crystallization could decrease from 6.41 min to 1.27 min at crystallization temperature of 105 °C while the crystallinity was increased to 50.0%. Non-isothermal crystallization of PLLA/furan-phosphamide composites further showed that, with increasing of furan-phosphamide loading, PLLA/furan-phosphamide composites had lower activation energy values, implying easier transformation for PLLA chains from molten into crystallization. Even then, the nucleation effect of current nucleating agents for PLLA still cannot reach nucleating aptitude of commercial nucleating agents for other polymers such as polyethylene terephthalate, polyethylene and polypropylene, as a result, a considerable number of organic nucleating agents with different structures need to be constructed to systematically explore the key structure and its structure-activity relationship affecting PLLA's crystallization which is one basic issue to develop new efficient organic nucleator. For this, an organic low molecular compound *N, N'*-bis(2-picolinyl) 1, 4-naphthalenedicarboxylic acid dihydrazide (designated in the current work as NCAPH) was employed to service as a new organic nucleating agent for the crystallization of PLLA, and the modified PLLA with various NCAPH loading from 0.5 to 3 wt% were fabricated using the melt blending technology, and then a comparative study on crystallization behaviors of the virgin PLLA and NCAPH-nucleated PLLA were evaluated through DSC and POM measurements; and then the various melting behaviors of the NCAPH-nucleated PLLA, including influences of the crystallization time, heating rate and crystallization temperature, were studied in detailed. This study is significant to further broaden the category of PLLA nucleating agent and reveal the related nucleation mechanism.

2. Materials and methods

Reagents and materials

NCAPH in the current work was prepared in our lab, and the main reagents for synthesizing NCAPH, including 2-picolinyl hydrazide, *N, N*-dimethylformamide, 1, 4-naphthalenedicarboxylic acid and thionyl chloride, were purchased from Shanghai Titan Scientific Co., Ltd, China. PLLA named 4032D produced by Nature-Works LLC was obtained from Dansheng Plastic, China.

Synthesis of NCAPH

NCAPH's synthesis pathway is shown in Figure.1. The synthetic procedure is similar to that of other compounds reported by our research group [32, 40], and there are two main reaction steps, they are acylation and amination reaction. The resulting NCAPH is characterized by ¹H Nuclear Magnetic Resonance (¹H NMR) and Fourier Transform Infrared Spectrometer (FT-IR), the detailed characterization data are as follows: FT-IR (KBr) ν : 3379.9 cm⁻¹ (the stretching vibrations absorption of N-H), 3257.7 cm⁻¹ (C-H stretching vibration of 2-pyridine), 1678.1 cm⁻¹ (the stretching vibration absorption of C=O which is near naphthalene), 1652.4 cm⁻¹ (the stretching vibration absorption of C=O which is near 2-pyridine), 1590.7, 1570.3, 1490 and 1464.1 cm⁻¹ (the vibration absorption of C-C of naphthalene and pyridine), 1515.6 cm⁻¹ (N-H bending vibration absorption), 1328.7 cm⁻¹ (the mixed absorption about bending vibration of N-H and stretching vibration of C-N), 1140.7 cm⁻¹ (the stretching vibration of C-H of naphthalene), 998.5 cm⁻¹ (the stretching vibrations absorption of C-C which located in C=O and naphthalene), 859.2 cm⁻¹ (the out-of-plane bending vibration absorption of C-H of naphthalene). ¹H NMR (400 MHz) δ : ppm; 11.04 (s, 1H, NH), 10.72 (s, 1H, NH), 8.84~9.30 (m, 4H, Py), 8.47~8.50 (m, 1H, Naphth), 7.69~7.76 (m, 2H, Naphth)).

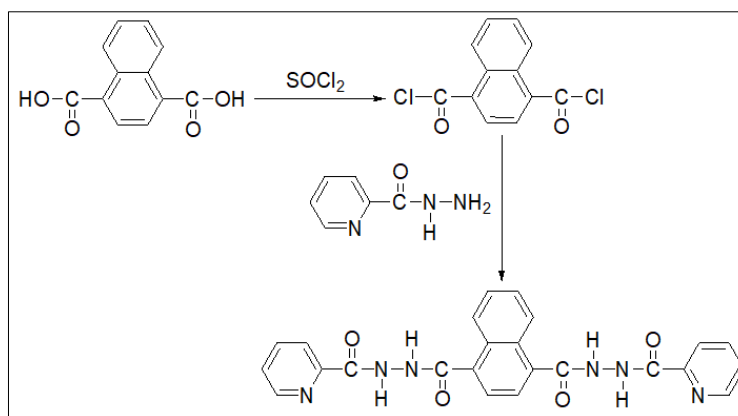


Figure 1. The schematic representation of the NCAPH synthesis pathway

Additionally, the geometry optimization of NCAPH was further performed by DMol3 modules, and the optimized geometry and electron density are presented in Figure 2. As exhibited in Figure 2, the amide group of NCAPH exhibits a relative low electron density, implying that, in comparison to other groups of NCAPH, the amide group maybe easy to interact with the high electron group from other molecule.

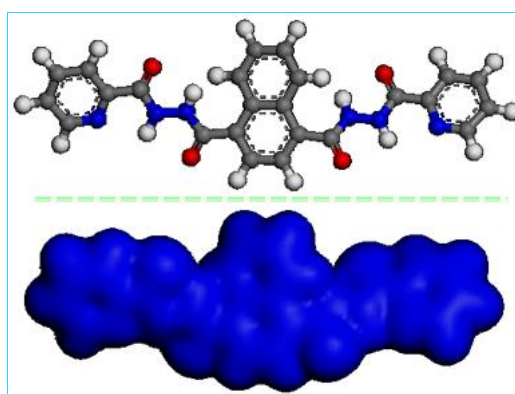


Figure 2. Optimum geometry and electron density of NCAPH

Preparation of PLLA/NCAPH

The virgin PLLA pellets and NCAPH were further dried at 45°C under vacuum for 24 h before melting blend. After that, the NCAPH was ground to ensure relatively good dispersion in PLLA, and then blends of NCAPH and PLLA were carried out in a counter-rotating mixer at 190°C with a 32 rpm rotor speed for 5 min and 64 rpm for 5 min. The modified PLLA with various amounts of NCAPH (the loading is 0.5 wt%, 1 wt%, 2 wt% and 3 wt%, respectively) were prepared. All PLLA/NCAPH were then converted into sheets by hot pressing at 20 MPa and 190°C for 5 min, and cool pressing at room temperature in square mold with a thickness of 0.4 mm. The virgin PLLA was also processed in the same way to obtain a reference material.

Characterization and test

NCAPH's structural characterization: NCAPH's molecular structure was determined by IS50 FT-IR (Thermo Fisher Scientific, USA) and ¹H NMR (Bruker, USA). For FT-IR characterization, a small amount of NCAPH powder was firstly blended with KBr, and then the mixture was ground to prepare testing sample through tableting method, and the wavenumber of FT-IR test was set from 4000 cm⁻¹ to 400 cm⁻¹. For ¹H NMR test, the dimethyl sulfoxide as deuterium reagent was selected to dissolve solid NCAPH.

Crystallization and melting behavior: Melt-crystallization processes and melting processes of the virgin PLLA and PLLA/NCAPH were recorded by DSC (Q2000, TA Instrument, USA). For melt-crystallization, a given tested sample was firstly heated to 180°C or 185°C or 190°C as different final melting temperature, and held at the final melting temperature for 3 min to eliminate thermal history, and then cooled at different rates, and the DSC curve was recorded to further analyze. For melting behavior, a given PLLA/NCAPH sample was still heated to 190°C for 3 min to ensure that PLLA/NCAPH crystals were melted completely, then the related melting process test was performed according to the set testing procedure.

Polarization optical microscopy (POM): The crystal morphology and crystal growth of the virgin PLLA and PLLA/NCAPH was observed using DPT200ia POM (UOP, China), and crystallization temperature was at 130°C.

3. Result and discussions

Crystallization behavior

This study is aimed at evaluating the influence of NCAPH on PLLA's crystallization, thus, the nucleating aptitude of NCAPH was firstly examined *via* non-isothermal melt-crystallization process. Figure 3 shows DSC cooling curves for the virgin PLLA and PLLA/NCAPH at a cooling rate of 1°C/min from the melt of 190°C. As observed, the virgin PLLA exhibits no discernible melt-crystallization peak in DSC cooling curve, showing its poor crystallization ability, which is thought to be because of the intrinsically tardy movement of the chains [41]. By contrast, when NCAPH is added into PLLA, they show different effects on PLLA's melt-crystallization behavior, that is, any PLLA/NCAPH has a remarkable and sharp exothermic peak, revealing that NCAPH could be used as an effective heterogeneous nucleation site for the crystallization of PLLA. Additionally, PLLA/NCAPH exhibits different melt-crystallization behaviors as NCAPH loading increased from 0.5 wt% to 3 wt%, meaning that NCAPH loading is an important factor for affecting PLLA's melt-crystallization. As seen in Fig.3, the melt-crystallization peak becomes sharper and shifts to the high-temperature side with increasing of NCAPH loading, indicating that a relative high NCAPH loading is beneficial for crystallization of PLLA, because the sharper melt-crystallization peak often represents the faster crystallization rate, the appearance of melt-crystallization peak located at higher temperature often also means better nucleation effect [42]. Specifically, as seen in Table 1, upon the addition of 2 wt% NCAPH, the onset crystallization temperature (T_o) has the highest value of 139.5°C, and the difference (ΔT) between T_o and the crystallization peak temperature (T_p) is the minimum value of , as well as the crystallization enthalpy (ΔH) has the maximum value of 48.5 J/g, showing that the crystallinity (X_c) of PLLA/2%NCAPH is 53.2% through the correlation equation [43].

However, it should be noted that, when NCAPH loading increases to 3 wt%, the non-isothermal melt-crystallization peak with a greater width shifts toward low-temperature side, which implies that an overdose of NCAPH loading have an inhibition for PLLA's non-isothermal melt-crystallization behavior, because an overdose of NCAPH loading blocked the mobility of PLLA molecular chain in cooling, further leading to slow crystal growth, which is also the main reason for wide melt-crystallization peak in DSC curve.

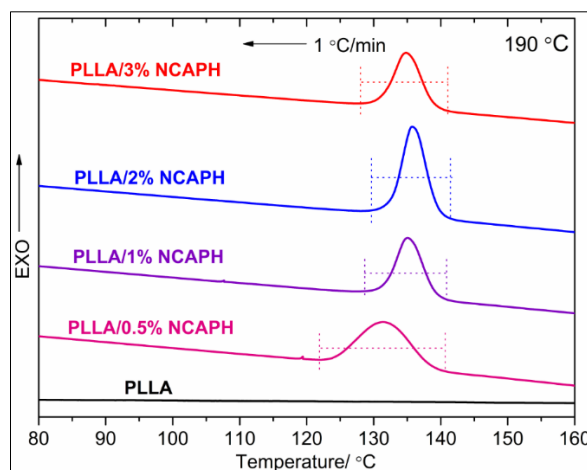


Figure 3. Melt-crystallization DSC curves of the virgin PLLA and PLLA/NCAPH at 1°C/min in cooling

Table 1. DSC data of PLLA/NCAPH at 1°C/min in cooling

Sample	T_0 / °C	T_p / °C	ΔT / °C	ΔH / J·g ⁻¹	X_c / %
PLLA/0.5% NCAPH	138.6	131.6	7.0	47.1	50.9
PLLA/1% NCAPH	139.2	135.1	4.1	46.9	50.9
PLLA/2% NCAPH	139.5	135.8	3.7	48.5	53.2
PLLA/3% NCAPH	139.0	134.9	4.1	47.7	52.9

Figure 4 and Figure 5 show effects of different cooling rates and final melting temperatures (T_f) on PLLA's melt-crystallization processes in cooling, respectively. As seen in Figure 4, the influence of NCAPH loading on PLLA's melt-crystallization cannot almost depend on the cooling rate, however, for any given PLLA/NCAPH, an increase of cooling rate leads to a wider non-isothermal melt-crystallization peak located at lower temperature, especially the melt-crystallization peak exhibits significant difference in peak width when increasing cooling rate from 2.5 to 5°C, indicating that the cooling rate is another key factor for affecting PLLA's melt-crystallization process, similar phenomena can be easily found in literatures [44, 45], and this result is considered to be caused by the following reason: at a relative slow cooling rate, there is sufficient time for the activation of the nuclei at a higher temperature; on the contrary, at a faster cooling rate, there is inadequate time for the activation of the nuclei [46], finally the crystallization only occurs at a low temperature. Additionally, as the cooling rate increases, the crystal growth takes more time to complete, resulting in wide melt-crystallization peak.

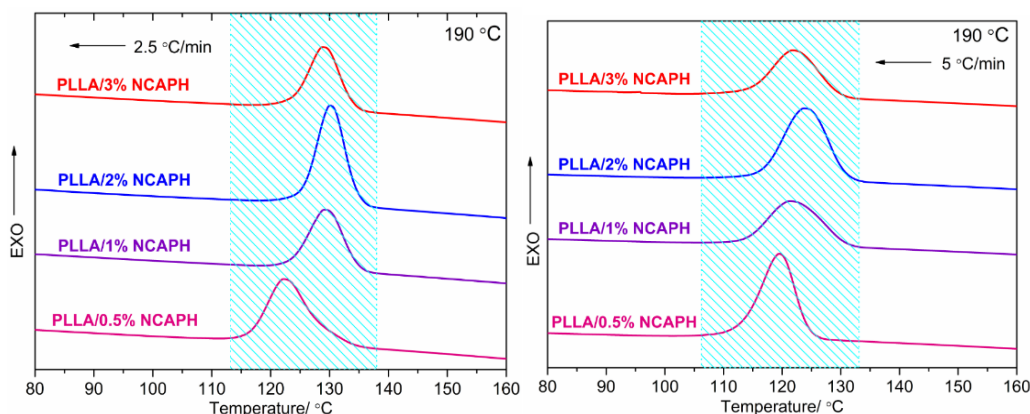


Figure 4. Non-isothermal melt-crystallization of PLLA/NCAPH at different cooling rates in cooling

Although T_f is different, the influence trend of NCAPH loading on non-isothermal melt-crystallization behavior of PLLA is consistent as shown in Figure 5. For a given PLLA/NCAPH, the different T_f can cause the melt-crystallization peak to appear in different temperature region. Through observation, it is found that, when T_f is 185°C, the non-isothermal melt-crystallization occur fastest and the non-isothermal melt-crystallization peak is also the sharpest, that is to say, 185°C is the optimum T_f comparing with other T_f of 180°C or 190°C, which may result from the competitive relationship between dissolved NCAPH and undissolved NCAPH, on one hand, a relatively small amount of NCAPH must be dissolved in PLLA resin, when PLLA/NCAPH is melted at T_f , and these dissolved NCAPH can enhance the interaction between PLLA and undissolved NCAPH, which is be beneficial for PLLA molecular segment to adhere to undissolved NCAPH surface to accelerate crystallization, and this effect becomes more significant as dissolved NCAPH concentration increases; However, on the other hand, an increase of dissolved NCAPH loading must lead to a drop in undissolved NCAPH concentration which determines nucleation density in PLLA matrix.

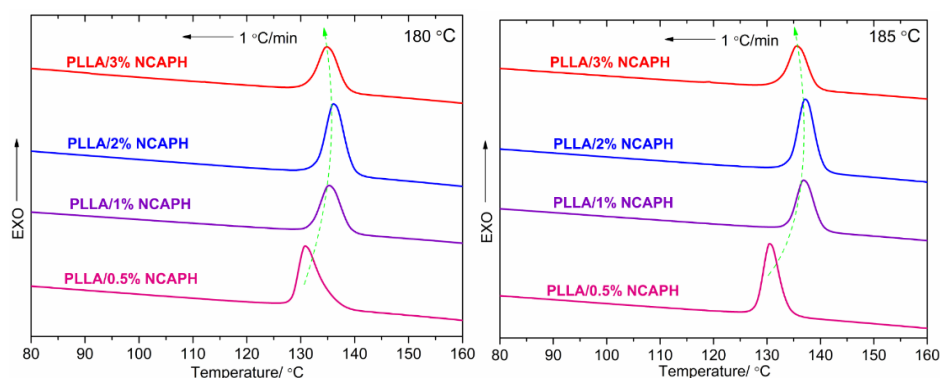


Figure 5. Non-isothermal melt-crystallization of PLLA/NCAPH at 1°C/min in cooling from different T_f

The crystal morphology of PLLA containing 0.5 wt% NCAPH was compared with that of the virgin PLLA through POM. POM images of the virgin PLLA and PLLA/0.5%NCAPH during isothermal crystallization process at 130°C was displayed in Figure 6. It is very clear that the virgin PLLA exhibited typical spherulite structure in Figure 6, and that the spherulite density is still very small after isothermal crystallization for 300 s. In contrast, PLLA/0.5%NCAPH can exhibit higher spherulite density after isothermal crystallization for only 90 s, further proving that NCAPH has efficient nucleation capability for PLLA's crystallization. During the crystallization's latter stages, the spherulite number further increases and spherulite size also becomes larger, but POM image shows that spherulite of the virgin PLLA cannot still pervade the entire image after crystallization for 600 s, showing the virgin PLLA's poor crystallization ability again. For PLLA/0.5%NCAPH sample, the spherulites impinge on their neighbors, and the spherulites form structures that pervade the entire image. In addition, it can be observed that the virgin PLLA's spherulite size is much larger than PLLA/0.5%NCAPH, the reason is that the spherulites are fully grown in space, when spherulite density is relative low.

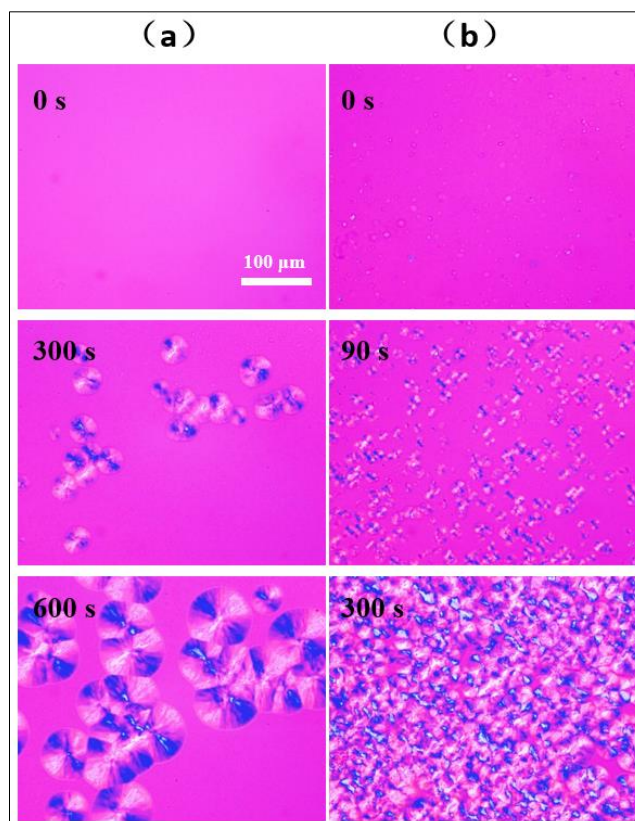


Figure 6. POM images of the virgin PLLA and PLLA/0.5%NCAPH after crystallization at 130°C (a: the virgin PLLA, b: PLLA/0.5%NCAPH)

The epitaxial nucleation and chemical nucleation are often used to explain nucleating agent's effect mechanism for polymer crystallization [47], for the current study, a theoretical calculation is performed to speculate the probable nucleation mechanism. Figure 7 is the lowest unoccupied molecular orbital (LUMO) and highest occupied molecular orbital (HOMO) of NCAPH and PLLA with ten units, respectively; and LUMO energy and HOMO energy of NCAPH are -0.110839 eV and -0.19941 eV, and LUMO energy and HOMO energy are 0.251 eV and -11.082 eV for PLLA. It is a fact that the energy gap between LUMO of NCAPH and HOMO of PLLA is lower than the LUMO-HOMO of PLLA itself. According to the frontier orbital theory, a smaller energy gap between LUMO and HOMO often means that the electron transition from HOMO to LUMO becomes easier, implying that the PLLA's HOMO electron easier flows to NCAPH's LUMO, especially when PLLA and NCAPH are melt blended, under this circumstance, PLLA and NCAPH have high molecular activity. Additionally, according to NCAPH's electron density (Figure 2), the intermolecular interaction is presumed to occur at N-H of NCAPH and C=O of PLLA, which is proved by other research group [48].

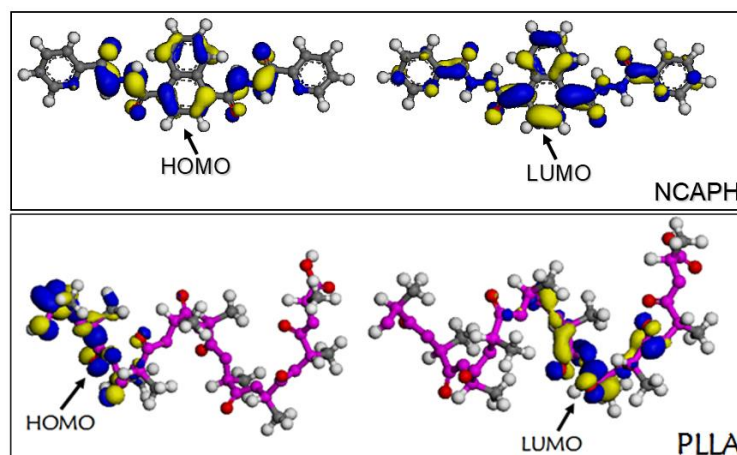
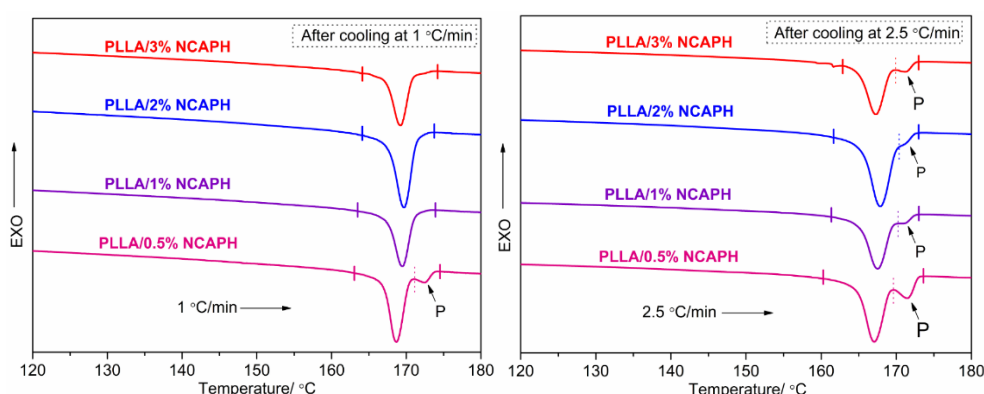


Figure 7. The frontier orbital of NCAPH and PLLA

Melting behavior

Figure 8 shows DSC thermograms at different heating rates that corresponded to the rates of non-isothermal melt-crystallization at different cooling rates. When the rate is $1^{\circ}\text{C}/\text{min}$, the double melting peaks are observed for only PLLA/0.5%NCAPH, however, the double melting peaks are observed for all PLLA/NCAPH as the rate increases, and the double melting peaks shift slightly to lower temperature side along with an increase in the rate, as well as melting peak significantly become wide. On one hand, this resultant reflects melt-crystallization before subsequent melting procedure, because a relative low cooling rate can promote PLLA/NCAPH's crystallization as seen in Figure 4, and the crystallization can be completed as far as possible in cooling when enough NCAPH loading can ensure high nucleation rate of PLLA, whereas the crystallization of PLLA with a small amount of NCAPH is insufficient in cooling, as a result, the double melting peaks appear in heating DSC curves. On the other hand, for cooling procedure or heating procedure, there is no enough time to form crystal with increasing of rate, which results in a shift toward low temperature side of melting peak, because the PLLA's melting temperature is directly correlative with perfection of crystal, usually, the higher the perfection of crystal is, the higher the melting temperature is. Furthermore, it is also observed from Figure 8 that the area ratio between low-temperature side melting peak and high-temperature side melting peak become small as the rate increased from $2.5^{\circ}\text{C}/\text{min}$ to $10^{\circ}\text{C}/\text{min}$, showing that the rate is an key factor for both melt-crystallization and melting behavior.



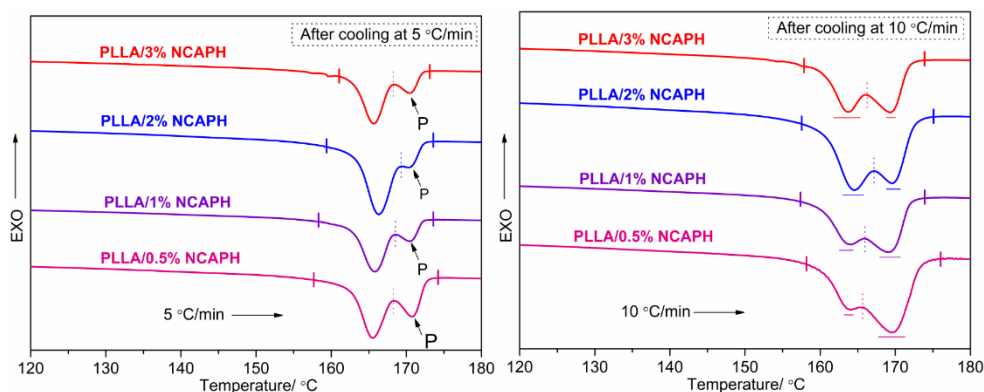


Figure 8. DSC thermograms of PLLA/NCAPH at different heating rates that corresponded to the rates of melt-crystallization at different cooling rates

The melting behaviors of PLLA/NCAPH after isothermal crystallization was also studied by DSC. DSC thermograms of PLLA with various NCAPH loading at a heating rate of 10 °C/min after isothermal crystallization at 125°C, 130°C and 135°C for different time (60 min, 120 min and 180 min) were shown in Figure 9. When the crystallization time is higher than 60 min, the influence of crystallization time on DSC melting curve of a given PLLA/NCAPH with the same crystallization temperature is negligible as shown in Figure 9, meaning that 60 min is enough time to complete PLLA's crystallization at related crystallization temperature. However, a higher crystallization temperature can make the melting peak slightly moves toward the higher-temperature side, the probable reason is that a relative high crystallization temperature can cause PLLA crystal to grow more perfect.

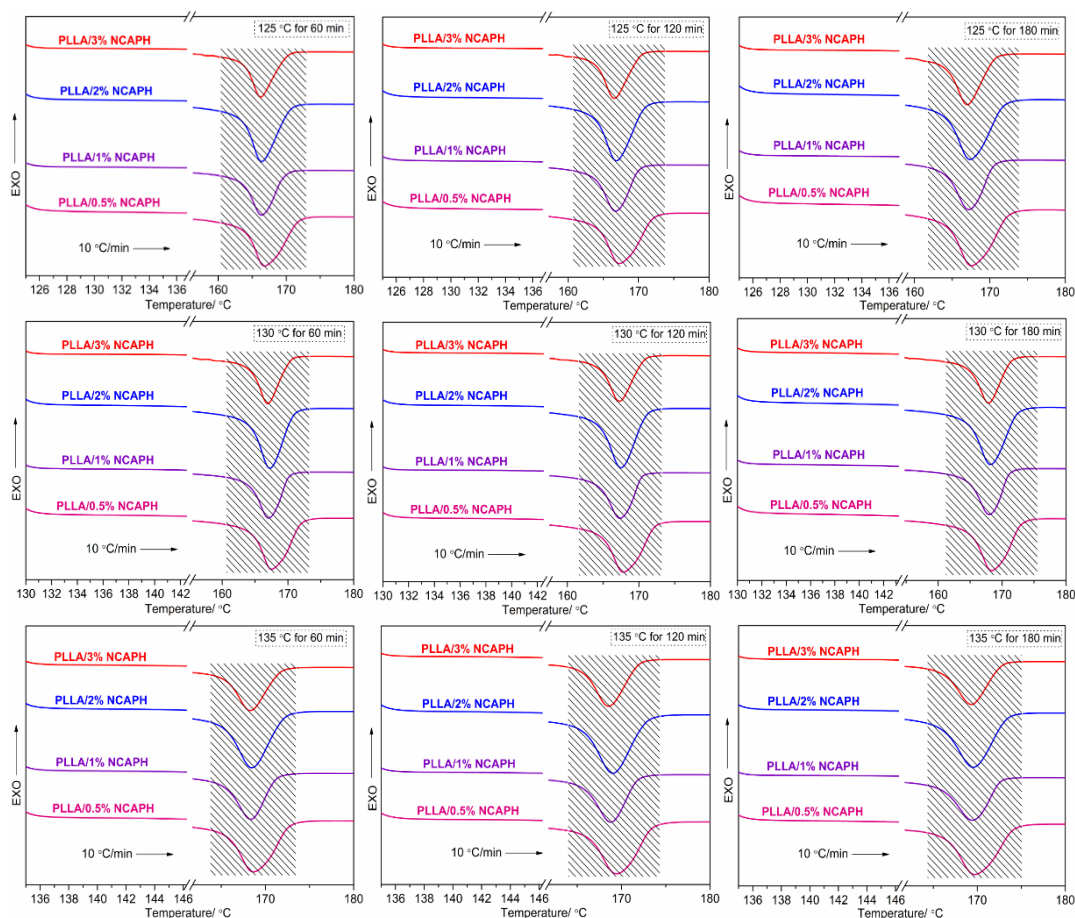
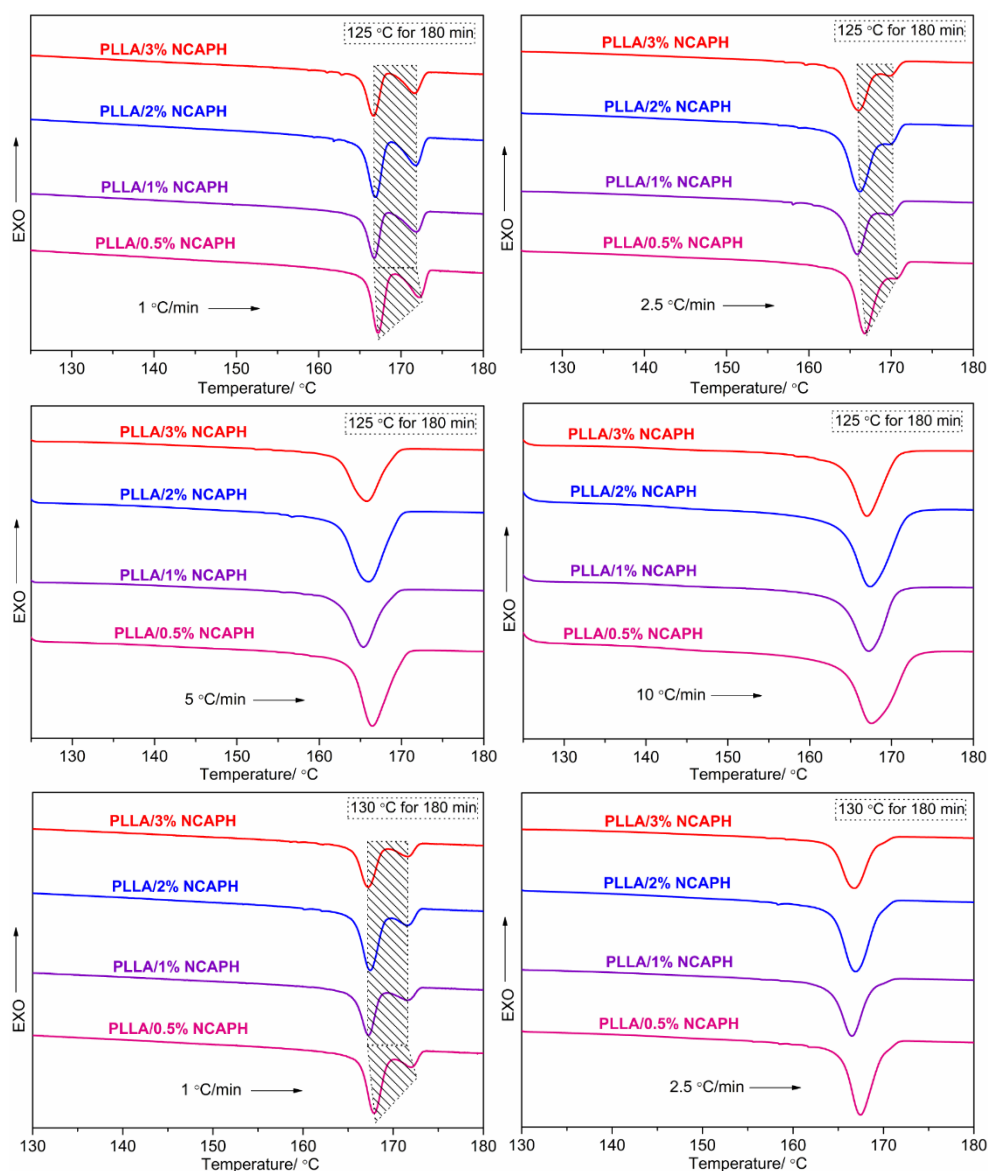


Figure 9. Melting behaviors of PLLA/NCAPH at 10°C/min in heating after isothermal crystallization at different crystallization temperatures for different time

As aforementioned, the heating rate affected PLLA/NCAPH's melting behaviors, further the influence of the heating rate on PLLA/NCAPH's melting process after sufficient crystallization was also investigated as shown in Figure 10. In view of the resultant of Figure 9, the crystallization time in this section was set to 180 min to ensure PLLA's sufficient crystallization as far as possible. When the heating rate is 1°C/min, double melting peaks can be clearly observed in DSC curves; and apart from PLLA/0.5%NCAPH, other PLLA/NCAPH samples have the same melting points of high-temperature side melting peak or low-temperature side melting peak at the same test level, showing that the melting temperature is irrelevant with NCAPH loading to some extent. However, when the heating rate is higher than 1°C/min, double melting peaks can appear only when the crystallization temperature is 125°C and the heating rate is 2.5°C/min, suggesting that the crystallization cannot still sufficiently complete at a relative low crystallization temperature, although the crystallization time is enough long, additionally, a slow heating rate is also beneficial for recrystallizing during the heating.



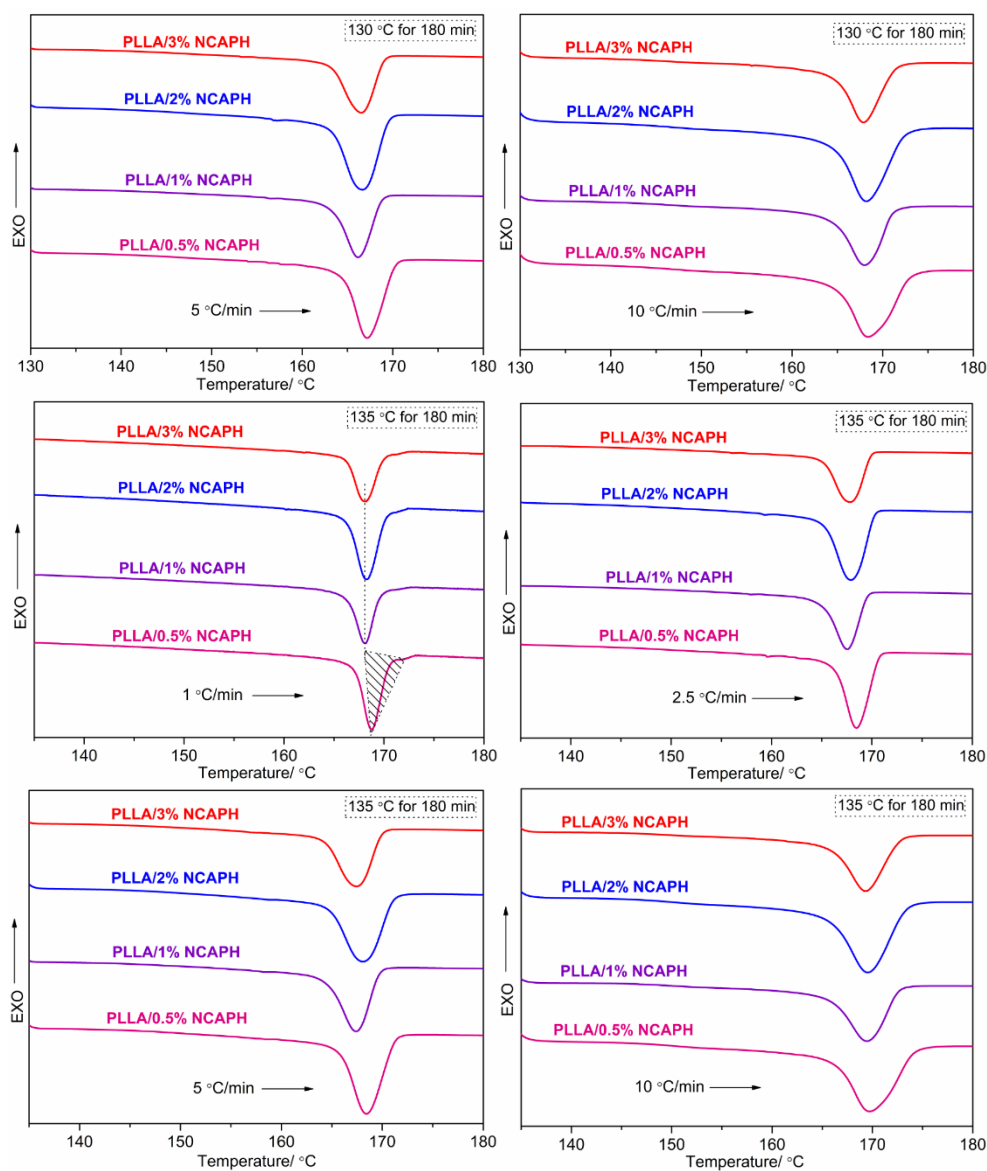


Figure 10. DSC Melting curves of PLLA/NCAPH at different heating rates after crystallization at different temperatures for 180 min

4. Conclusions

NCAPH was developed to evaluate its influence on PLLA's crystallization and melting process through DSC and POM tests. The melt-crystallization indicated that the virgin PLLA's crystallization ability was very poor, whereas the introduction of NCAPH significantly enhanced crystallization ability of PLLA, which be proved *via* the appearance of sharp crystallization peak in cooling. And for melt-crystallization behaviors, the cooling rate and T_f were two other key factors for affecting PLLA's melt-crystallization process, and the crystallization ability of a given PLLA/NCAPH was weakened as cooling rate increased; and through comparative analysis, it is found that 185°C was the optimum T_f , because the sharpest melt-crystallization peak appeared in cooling DSC curve. Additionally, POM testing results further confirmed crystallization promoting effect of NCAPH for PLLA due to a large increase in spherulite density per unit volume. This influence of NCAPH for PLLA's crystallization was attributed to chemical nucleation *via* the primary theoretical analysis. For PLLA/NCAPH's melting process, the difference in melting behavior resulted from the effects of the crystallization time, heating rate and NCAPH loading after crystallization, because these influence factors changed PLLA's crystallization, hence the final melting behavior must depend on the crystallization.



Acknowledgements: This study was supported by Foundation of Chongqing Science and Technology Bureau, Scientific and Technological Research Program of Chongqing Municipal Education Commission, and Chongqing University of Arts and Sciences (project number P2020HH06 and Y2022HH02).

References

1. ROY M., ZHELEZNIAKOV M., DE KORT G.W., HAWKE L.G.D., LEONE N., RASTOGI S., Wilsens CHRM. On the nucleation of polylactide by melt-soluble oxalamide based organic compounds [J], *Polymer*, 2020, 202: 122680
2. CHEN W.W., QI C.Z., LI Y., TAO H.Y., The degradation investigation of biodegradable PLA/PBAT blend: Thermal stability, mechanical properties and PALS analysis [J], *Radiation Physics and Chemistry*, 2021, 180: 109239
3. KUANG J., WANG J.H., BAI Y., LI Y.C., Effects and mechanism of cellulose acetate butyrate on the crystallization of polylactic acid [J], *European Polymer Journal*, 2019, 121: 109286
4. SWAROOP C., SHUKLA M., Development of blown polylactic acid-MgO nanocomposite films for food packaging [J], *Composites Part A*, 2019, 124: 105482
5. DU M.X., JARIYAVIDYANONT K., BOLDT R., TARIQ M., FISCHER M., SPOERER Y., KUEHNERT I., ANDROSCH R., Crystal-nuclei formation during injection-molding of poly (L-lactic acid) [J], *Polymer*, 2022, 250: 124897
6. LI X.L., WANG R., YANG C.F., DONG Z.F., ZHANG X.Q., WANG D.J., WANG D.Y., Effect of Poly(D-lactic acid) block copolymers with soft chains on the tensile behavior of Poly(L-lactic acid) [J], *Acta Polymerica Sinica*, 2018, 5: 598-606
7. WANG F., NAN Z., SUN X.L., LIU C., ZHUANG Y., ZAN J.A., DAI C.F., LIU Y.F., Characterization of degradation behaviors of PLA biodegradable plastics by infrared spectroscopy [J], *Spectrochimica Acta Part A-Molecular and Biomolecular Spectroscopy*, 2022, 279: 121376
8. TANG X.L., DUAN W.M., YANG M., XU K., ZHENG C.C., Construction and degradation mechanism of polylactic acid-pH-responsive microgel composite system plugging system [J], *Journal of Dispersion Science and Technology*, 2022, DOI10.1080/01932691.2022.2106996
9. EBRAHIMIFAR M., TAHERIMEHR M., Evaluation of in-vitro drug release of polyvinylcyclohexane carbonate as a CO₂-derived degradable polymer blended with PLA and PCL as drug carriers [J], *Journal of Drug Delivery Science and Technology*, 2021, 63: 102491
10. ZHANG Y.Y., WEN Q.Z., ZHANG D.X., A novel targeted plugging and fracture-adaptable gel used as a diverting agent in fracturing [J], *Energy Science & Engineering*, 2020, 8(1): 116-133
11. HE Z.J., SHAO H.F., ZHANG N.N., LI J., XIAO H., WENG T.H., ZHOU M., WEN B.Y., CHEN Y.L., The crystalline behavior of poly(L-lactide) induced by nucleating agents with amide structure: The effect of benzamide molecule symmetry [J], *Journal of Polymer Science*, 2022, DOI: 10.1002/pol.20220295
12. ZHANG B., BIAN X.C., XIANG S., LI G., CHEN X.S., Synthesis of PLLA-based block copolymers for improving melt strength and toughness of PLLA by in situ reactive blending [J], *Polymer Degradation and Stability*, 2017, 136: 58-70
13. SHI D.W., LAI X.L., JIANG Y.P., YAN C., LIU Z.Y., YANG W., YANG M.B., Synthesis of inorganic silica grafted three-arm PLLA and their behaviors for PLA Matrix [J], *Chinese Journal of Polymer Science*, 2019, 37(3): 216-226
14. TANG Y.J., WANG Y.Q., CHEN S.H., WANG X.D., Fabrication of low-density poly(lactic acid) microcellular foam by self-assembly crystallization nucleating agent [J], *Polymer Degradation and Stability*, 2022, 198: 109891
15. KHWANPIPAT T., SEADAN M., SUTTIRUENGWONG S., Effect of PDLA and amide compounds as mixed nucleating agents on crystallization behaviors of Poly (L-lactic acid) [J], *Materials*, 2018, 11(7): 1139



- 16.LI C.H., LUO S.S., WANG J.F., WU H., GUO S.Y., ZHANG X., Conformational regulation and crystalline manipulation of PLLA through a self-assembly nucleator [J], *Biomacromolecules*, 2017, 18(4): 1440-1448
- 17.ZHANG H.H., WANG S.J., ZHANG S.Y., MA R.X., WANG Y.M., CAO W., LIU C.T., SHEN C.Y., Crystallization behavior of poly(lactic acid) with a self-assembly aryl amide nucleating agent probed by real-time infrared spectroscopy and X-ray diffraction [J], *Polymer Testing*, 2018, 64: 12-19
- 18.XING Q., ZHANG X.Q., DONG X., LIU G.M., WANG D.J., Low-molecular weight aliphatic amides as nucleating agents for poly (L-lactic acid): Conformation variation induced crystallization enhancement [J], *Polymer*, 2012, 53(11): 2306-2314
- 19.MA P.M., XU Y.S., SHEN T.F., DONG W.F., CHEN M.Q., LEMSTRA P.J., Tailoring the crystallization behavior of poly(L-lactide) with self-assembly-type oxalamide compounds as nucleators: 1. Effect of terminal configuration of the nucleators [J], *European Polymer Journal*, 2015, 70: 400-411
- 20.COPPOLA B., CAPPETTI N., DI MAIO L., SCARFATO P., INCARNATO L., 3D Printing of PLA/clay nanocomposites: influence of printing temperature on printed samples properties [J], *Materials*, 2018, 11(10): 1947
- 21.XU Z.B., SU L.Y., JIANG S.C., GU W., PENG M., WANG P.F., Crystallization behavior and water vapor permeability of poly(lactic acid) nanocomposite under oscillatory shear [J], *Journal of Applied Polymer Science*, 2015, 132(30): 42321
- 22.JIANG G., HUANG H.X., CHEN Z.K., Microstructure and thermal behavior of polylactide/clay nanocomposites melt compounded under supercritical CO₂ [J], *Advances in Polymer Technology*, 2011, 30(3): 174-182
- 23.LI Y., HAN C.Y., YU Y.C., XIAO L.G., SHAO Y., Effect of content and particle size of talc on nonisothermal melt crystallization behavior of poly(L-lactide) [J], *Journal of Thermal Analysis and Calorimetry*, 2019, 135(4): 2049-2058
- 24.D'URSO L., ACOCELLA M.R., DE SANTIS F., GUERRA G., PANTANI R., Poly(L-lactic acid) nucleation by alkylated carbon black [J], *Polymer*, 2022, 256: 125237
- 25.NING N.Y., ZHANG W., ZHAO Y.S., LUO F., FU Q., Nanohybrid shish kebab structure and its effect on mechanical properties in poly(L-lactide)/carbon nanotube nanocomposite fibers [J], *Polymer International*, 2012, 61(11): 1634-1639
- 26.XU J.Z., CHEN T., YANG C.L., LI Z.M., MAO Y.M., ZENG B.Q., Hsiao BS. Isothermal crystallization of Poly(L-lactide) induced by graphene nanosheets and carbon nanotubes: A comparative study [J], *Macromolecules*, 2010, 43(11): 5000-5008
- 27.TSUJI H., KAWASHIMA Y., TAKIKAWA H., TANAKA S., Poly(L-lactide)/nano-structured carbon composites: Conductivity, thermal properties, crystallization, and biodegradation [J], *Polymer*, 2007, 48(14): 4213-4225
- 28.HAN L.J., HAN C.Y., BIAN J.J., BIAN Y.J., LIN H.J., WANG X.M., ZHANG H.L., DONG L.S., Preparation and characteristics of a novel nano-sized calcium carbonate (nano-CaCO₃)-supported nucleating agent of poly(L-lactide) [J], *Polymer Engineering and Science*, 2012, 52(7): 1474-1484
- 29.RASHIDI H., OSHANI B.N., HEJAZI I., SEYFI J., Tuning crystallization and hydrolytic degradation behaviors of poly(lactic acid) by using silver phosphate, zinc oxide and their nano-hybrids [J], *Polymer-Plastics Technology and Materials*, 2020, 59(1): 72-82
- 30.WANG S.S., HAN C.Y., BIAN J.J., HAN L.J., WANG X.M., DONG L.S., Morphology, crystallization and enzymatic hydrolysis of poly(L-lactide) nucleated using layered metal phosphonates [J], *Polymer international*, 2011, 60(2): 284-295
- 31.CAI Y.H., TANG Y., ZHAO L.S., Poly(L-lactic acid) with the organic nucleating agent *N,N,N'*-tris(1H-benzotriazole) trimesinic acid acethydrazide: Crystallization and melting behavior [J], *Journal of Applied Polymer Science*, 2015, 132: 42402
- 32.CAI Y.H., ZHAO L.S., TIAN L.L., Investigating the crystallization, melting behavior, and thermal stability of poly(L-lactic acid) using aromatic isoniazid derivative as nucleating agent [J], *Polymer Bulletin*, 2017, 74: 3751-3764



33. ZHAO L.S., CAI Y.H., Investigating the physical properties of Poly(L-lactic acid) modified using an aromatics succinic dihydrazide derivative[J], *Polymer Science, Series A*, 2018, 60(6): 777-787
34. HUANG H., ZHANG Y.H., ZHAO L.S., LUO G.M., CAI Y.H., Insight into the role of a isophthalic dihydrazide derivative containing piperonylic acid in Poly(L-lactide) nucleation: Thermal performances and mechanical properties [J], *Mater. Plast.*, **57**(3), 2020, 28-40
35. ZHAO L.S., QIAO J., CHEN W., CAI Y.H., Thermal and mechanical properties of poly(L-lactic acid) nucleated with *N, N'*-bis(phenyl) 1,4-naphthalenedicarboxylic acid dihydrazide [J], *Polimery*, 2021, 66(4): 234-244
36. XIAO D., ZHENG M.T., WU F.J., CAO X.X., HUANG X.F., HUANG L., XIAO X.Q., Fabrication of novel renewable furan-based phosphorus and its applications in poly (lactic acid): Thermal, flammability, crystallization and mechanical properties [J], *Polymer Degradation and Stability*, 2022, 203: 110060
37. ROY M., ZHELEZNIAKOV M., DE KORT G.W., HAWKE L.G.D., LEONE N., RASTOGI S., Wilsens CHRM. On the nucleation of polylactide by melt-soluble oxalamide based organic compounds [J], *Polymer*, 2020, 202: 122680
38. LAI W.C., LIAO J.P., Nucleation and crystal growth kinetics of poly(L-lactic acid) with self-assembled DBS nanofibrils [J], *Materials Chemistry and Physics*, 2013, 139: 161-168
39. SUN J.H., LI L., LI J., Effects of furan-phosphamide derivative on flame retardancy and crystallization behaviors of poly(lactic acid) [J], *Chemical Engineering Journal*, 2019, 369: 150-160
40. HUANG H., CAI Y.H., ZHAO L.S., Thermal properties and processability of modified poly(L-lactide): The role of phenylacetic acid hydrazide derivative [J], *Polimery*, 2022, 67(9): 12-21
41. YAO J.Q., LUO F.L., MAO J., LI Y.T., LIU Y.D., SUN X.L., The effect of nanocrystalline ZnO with bare special crystal planes on the crystallization behavior, thermal stability and mechanical properties of PLLA [J], *Polymer Testing*, 2021, 100: 107244
42. SU Z.Z., GUO W.H., YONGJUN LIU Y.J., LI Q.Y., WU C.F., Non-isothermal crystallization kinetics of poly(lactic acid)/modified carbon black composite [J], *Polymer Bulletin*, 2009, 62: 629-642
43. ZHAO L.S., CAI Y.H., Non-isothermal Crystallization, Melting behavior, Thermal Decomposition, Fluidity and Mechanical Properties of Melt Processed Poly(L-lactic acid) Nucleated by *N, N'*-Adipic Bis(Piperonylic Acid) Dihydrazide[J], *Polymer Science, Series A*, 2020, 62(4): 343-353
44. SU Z.Z., LI Q.Y., LIU Y.J., GUO W.H., WU C.F., The nucleation eEffect of modified carbon black on crystallization of poly(lactic acid) [J], *Polymer Engineering and Science*, 2010, 50: 1658-1666
45. SHI Q.F., MOU H.Y., GAO L., YANG J., GUO W.H., Double-melting behavior of bamboo fiber/talc/poly (lactic acid) composites [J], *Journal of Polymers and The Environment*, 2010, 18(4): 567-575
46. LI S., XIONG Z.Y., FEI P., CAI J., XIONG H.G., TAN J., YU Y., Parameters characterizing the kinetics of the nonisothermal crystallization of thermoplastic starch/poly(lactic acid) composites as determined by differential scanning calorimetry [J], *Journal of Applied Polymer Science*, 2013, 129: 3566-3573
47. PAN P.P., LIANG Z.C., CAO A., INOUE Y., Layered metal phosphonate reinforced poly(L-lactide) composites with a highly enhanced crystallization rate [J], *ACS Applied Materials & Interfaces*, 2009, 1(2): 402-411
48. HE Z.J., SHAO H.F., ZHANG N.N., LI J., XIAO H., WENG T.H., ZHOU M., WEN B.Y., CHEN Y.L., The crystalline behavior of poly(L-lactide) induced by nucleating agents with amide structure: The effect of benzamide molecule symmetry [J], *Journal of Polymer Science*, 2023, 61(1): 67-82

Manuscript received: 26.12.2022